ISSN NO. 2320-5407

Journal homepage: http://www.journalijar.com

INTERNATIONAL JOURNAL OF ADVANCED RESEARCH

RESEARCH ARTICLE

EFFECT OF DOPANTS ON THE MORPHOLOGICAL, CRYSTALLINE DEFECT AND BIOLOGICAL ACTIVITY OF ALKALI, ALKALINE EARTH AND TRANSITION METAL IONS DOPED L-HISTIDINE SINGLE CRYSTALS

V. RENUGA*
Department of Chemistry, National College, Tiruchirappalli, Tamil Nadu

Manuscript Info

Manuscript History:

Received: 22 March 2014
Final Accepted: 25 April 2014
Published Online:May 2014

Key words:
Dopant, Defect, Powder XRD and Antimicrobial Study

Corresponding Author

V. RENUGA

Abstract

The semi-organic nonlinear optical crystals of pure and alkali, alkaline earth and transition metal ions doped L- Histidine single crystals were grown by slow evaporation solution growth technique. The effect of the dopant on the growth and morphology has been investigated. The grown crystals were analyzed by powder X-Ray diffraction, FT-IR spectral analysis and UV-visible absorption spectra. UV-visible absorption studies show that the grown crystals have wide optical transparency in the entire visible region. Effects of dopant on the crystal defect on the grown crystals were characterized by Optical Microscopy. Anti microbial study of the grown crystals were analyzed using gram positive and gram negative micro organisms.

1. Introduction

Recent studies indicate that the L-histidine favorably forms several salts with organic or inorganic acids. The amino acid viz. L-histidine serves as a proton donor, proton acceptor and as a nucleophilic reagent. L-histidine frequently occurs at the active sites of enzymes and co-ordinates ions on large protein structures[1].

The imidazole side chain of L-histidine is a common coordinating ligand in metalloproteins and is a part of catalytic sites in certain enzymes. In catalytic triads, the basic nitrogen of L-histidine is used to abstract a proton from serine, threonine, or cysteine to activate it as a nucleophile. In a histidine proton shuttle, L-histidine is used to quickly shuttle protons. It can do this by abstracting a proton with its basic nitrogen to make a positively charged intermediate and then use another molecule, a buffer, to extract the proton from its acidic nitrogen. In carbonic anhydrases, a L-histidine proton shuttle is utilized to rapidly shuttle protons away from a zinc-bound water molecule to quickly regenerate the active form of the enzyme.

In recent years the need of nonlinear optical single crystals are very much felt useful in the fields of second harmonic generation, fiber optic communication, electro-optic modulation etc[2,3]. The search for new materials with high optical nonlinearities is an important area due to their practical applications such as optical communication, optical computing, optical disc data storage, laser fusion reactions, remote sensing, color display, medical diagnostics etc.[4] L-Histidine contains an imidazole ring with 2 nitrogen atoms: one is basic and the other is not. The basic nitrogen is involved in the delocalization which is important during enzyme catalysis. Today L-histidine is widely recognized as an essential amino acid which cannot be formed by other nutrients, and therefore should be in the diet to let our body obtains it. Our body mostly needs[5] L-histidine to regulate and to utilize essential trace

elements like iron, copper, molybdenum, zinc, and manganese. This amino acid is also essential in forming numerous metal-bearing enzymes and compounds, such as the antioxidant super oxide dismutase.

Alkali and alkaline earth metal cations from the s-block elements of the periodic table play an important role in nature, for instance alkali cations Li^+, Na^+ and K^+ have very specific functions such as the regulation of the ionic equilibrium of living cells in our body. Alkaline earth cations also have a contribution in our body, for instance calcium is the most important constituent of our organism. Above all, and always, such crystals find applications in man-made materials in a wide range of fields such as catalysts, ferroelectrics, metallic conductors and superconductor materials.

The coordination chemistry of groups 1 and 2 metal compounds[6-9] with organic ligands in the widest sense has been, until relatively recently, largely unknown compared to transition metal coordination networks. This is true despite the fact that many s-block metal–organic compounds are already of commercial importance. Thus, pharmaceuticals, dyes, and pigments typically use alkali and/or alkaline earth metal cations in preference to transition or lanthanide metal ions because most of them have the advantage of being non-toxic, cheap and soluble in aqueous media. Indeed, s-block cations should not be ignored as simple "spectator" ions when it comes to properties which depend on the solid-state structure and the intermolecular interactions.

Based on the vast applications of L-Histidine the present study was concentrated on the synthesis of alkali, alkaline earth and transition metal ions doped L-Histidine to find out if there is any change in morphology or because of dopant if any defect exist in the L-Histidine amino acid. Moreover the presence of dopant also influences the biological activity of the L-Histidine amino acid. To find out this antimicrobial activity of the prepared doped L-Histidine experiments were carried out in the present study using two gram positive and two gram negative bacteria.

2. Experimental section

2.1 Solubility study of pure and metal ions doped L-histidine single crystals

Solubility study was carried out using a hotplate, magnetic stirrer and a digital thermometer. Initially, the temperature of solvent was maintained at 40^oC. The synthesized salt of L-histidine was added systematically to 100 ml of de-ionized water in an airtight container kept on the hot-plate magnetic stirrer and stirring was continued till a small precipitate was formed and this confirms the supersaturated condition of the solution. Then, 25 ml of the solution was pipetted out and taken in a petridish and it was warmed up to 40^oC till the solvent was completely evaporated and solubility was determined by gravimetrical method[9]. The same procedure was followed to find solubility of pure and metal ions doped L-histidine samples at other temperatures. Variation of solubility with temperature for pure and metal ions added L-histidine salts are presented in fig.1 it is observed from the results that the solubility increases with increase in temperature for both types of crystals and it is found to be more for metal ions doped L-histidine crystals compared to the undoped crystal.

The photographs of the prepared pure and metal ions doped L-Histidine crystals are shown in Fig.2

2.2 Synthesis of pure L-Histidine single crystal

The analytical grade L-histidine (99% pure) was taken as starting material to synthesize pure L-histidine single crystal. The calculated amount of L-histidine was dissolved in deionized water and stirred well for about 6 hrs at 40^oC at a constant rate to get homogeneity. Two drops of H_2O_2 were added to the mother solution to inhibit the growth of any microorganism. Prepared solution was then filtered twice using Whatmann filter paper. The solution was transferred to a petridish and it was allowed to evaporate isothermally at 40°C in a constant temperature water bath for few days to get optically good L-histidine single crystals with perfect external morphology and are harvested in a period of 45-50 days. The harvested crystals were washed several times with acetone and dried for further study.

2.3 Synthesis of metal ions doped L-Histidine single crystals

The metal ions doped L-histidine were synthesized from L-histidine and metal sulphates (Na^{2+}, K^{2+}, Mg^{2+}, Ni^{2+}, Cu^{2+}, Zn^{2+}) (AR grade) in the ratio 1: 1. The reactants were dissolved in the deionised water and stirred well for about 6 hrs at 40^oC. Two drops of H_2O_2 were added to the mother solution to inhibit the growth of any micro-organism. Prepared solution was then filtered twice using Whatmann filter paper, the solution was transferred to a petridish and it was allowed to evaporate isothermally at 40°C in a constant temperature water bath for few days to get optically good metals doped L-histidine single crystals with perfect external morphology and were harvested

within a period of 45-50 days. The harvested crystals were washed several times with acetone and dried for further study.

3. Results and Discussions

3.1 FT-IR Spectral analysis of pure and metal ions doped L-Histidine single crystals

FTIR spectra of pure and metal ions doped L-Histidine are presented in fig.3.The L-histidine molecule is more basic and therefore the presence of NH_2^+ group is revealed in the FTIR spectrum that shows an intense band with strong absorption around 3445 cm^{-1} and protonated by the carboxyl group (COOH), giving hydrogen bonding interaction between NH_3^+ and COO^-. It is again confirmed that the amino and imidazole group are protonated and counter balance the negative charge of the carboxylate ions. The broad envelope band around 3000 to 2000 cm^{-1} is due to the superimposed O-H and NH_3^+ stretching vibrations. Absorption in this region is characterized by multiple fine structures in the low wave number region and it extends up to 2000 cm^{-1}. In the overtone region there is a prominent band near 2000 cm^{-1}, due to combination of the asymmetrical NH_3^+ bending vibration and the torsional oscillation of the NH_3^+ groups. The presence of NH_3^+ is identified corresponding to the asymmetric stretching mode of NH_3^+ and OH stretch of water molecule. The peaks at 1416 cm^{-1} are assigned to COO^- stretching vibrations. The peak at 1635 cm^{-1} gives rise to C=O stretching mode of vibrations. The assignments for peaks/bands are given in accordance with the data in the literature [10-13].

3.2 UV Spectra of pure and metal ions doped L-Histidine single crystals

UV-visible spectra of pure and metal ions doped L-histidine crystals are depicted in fig. 4. Optical absorption data were taken for the samples of thickness of about 2 mm. The material has a good optical absorption in the entire UV region and the lower cut off wavelength was observed at 218 nm and 212 nm for pure and metal ions doped L-histidine crystals and this is due to π - π^* transition in the compounds. The imidazole ring of L-histidine is aromatic at all pH values. It contains six pi electrons: four from two double bonds and two from a nitrogen lone pair. It can form pi stacking interactions, but is complicated by the positive charge. So it does not absorb at 280 nm in either state, but does in the lower UV range more than some amino acids.[14,15]

The band gap energy ($E_g = hc/\lambda$) was found to be 5.698 and 5.859 eV for pure and metal ions doped L-histidine crystals and thus ascertain the fact that the crystals are insulators and can be used for laser applications. The useful absorption range of pure and metal ions doped L-histidine crystals extends from 218 to 600 nm and which makes it very valuable for those applications requiring blue green light [16, 17].

3.3 Powder XRD analysis of pure and metal ions doped L-Histidine single crystals

In the present study, the powdered samples were analyzed by employing CuKα (λ=1.540598 Å) radiation of X-ray. The standard unit cell parameters of L-histidine were given as reference and the unit cell parameters for each sample were calculated by the software with assignment of different planes to Bragg reflections. Fig.5 presents the powder XRD patterns of pure and the different nature of metal ions doped L-histidine amino acid crystals and unit cell parameters of different samples are listed in table 1.

It can be inferred from fig.5 that the crystals figures exhibit almost the single phase nature. The doping of metal ions on amino acid does not bring large distortion in L-histidine crystal and it allows retaining of almost the single phase nature. In all doped samples, very little variation in the unit cell parameters is observed compared to pure L-histidine crystal; this may be due to larger amino acid molecules have adjusted inside interstitial voids instead of replacement of metal ions at any lattice point, the small variation in cell parameters can also be attributed to small strain on lattice [18,19]. Moreover, the synchrotron radiation X – ray multiple diffraction study of L-histidine phase transition induced by electric field has been reported by Santosh et al[20].The effect of doping on crystal structure of L-histidine and the presence of extra phase can be detected by powder XRD. From the XRD data investigation, it was found that lattice distortion took place in metal ions doped L-histidine crystals, and the structures of the doped crystals were slightly distorted compared to pure L-histidine crystal. This might be attributed to strains on the lattice by the absorption of metal ions prior to L-histidine crystal. The single phase nature after doping and shift in the peak positions with change in unit cell parameters are compiled and presented in table 1.

3.4 Etching studies of pure and metal ions doped L-Histidine

The chemical etching studies were carried out on the grown single crystals of L-histidine and metal ions doped L-histidine were done to study the symmetry of the crystal face from the shape of etch pit and the distribution of structural defects in the grown crystals. The (011) face of conventional grown L-histidine crystals were subjected to etching with water. The surface of the grown L-histidine single crystal was dipped for 10 sec in the water etchant for etching. The etched samples were dried using tissue paper and the etch patterns were observed using an optical microscope (Magnus MLX) [21]. Fig.6 represents etch pit patterns produced on the (011) face of the grown L-histidine crystal. The etch pits did not disappear upon continuous etching, suggesting that the pits were due to dislocations. Figure 6 shows the etch pits observed for the as grown L-histidine on the (011) face. In grown doped L- histidine

crystal the size of the etch pit is large compared to grown undoped L-histidine. The possible reasons for large size etch pits in doped L-histidine crystal may be due to the crystalline perfection. When the crystal was etched in an etchant the etch pit occurred more quickly in the region with less impurity contents. In utilizing single crystals for any applications it is essential to grow single crystals containing a reduced dislocation density. The most significant features of the dislocation structure were a tendency for certain dislocation types to nucleate in pairs and at growth sector boundaries. Among the numerous processes, which are influenced by crystallographic defects, there can be few situations in which the inter connections are as close as in the case of crystal growth.

Crystallization influences, and is influenced by, the defect structure of a crystal. Some of the dislocation pairs formed at isolated nucleation points originate at growth sector boundaries[22]. In L-histidine the faceted growth is avoided so that the growth sectors will be reduced. Hence the dislocations which are associated with growth sector boundaries are absent in L- histidine grown crystal. This is the reason for low dislocation density in L-histidine grown crystal. Decrease in etch pits is associated with more systematic packing of the atoms/molecules and the strains formed during growth.

3.5 Antimicrobial activity of pure and metal ions doped L-Histidine single crystals

According to the results of the antibacterial activity of L-histidine and the metal ions doped L-histidine showed antibacterial activity at 30°C and 37°C. In solution it is the nature of the amino acid R-groups that dictate structure-function relationships of peptides and proteins. The hydrophobic amino acids will generally be encountered in the interior of proteins shielded from direct contact with water. Conversely, the hydrophilic amino acids are generally found on the exterior of proteins as well as in the active centers of enzymatically active proteins. Indeed it is the very nature of certain amino acid R- groups that allow enzyme reactions to occur.

The imidazole ring of L-histidine allows it to act as either a proton donor or acceptor at physiological pH. Hence it is frequently found in the reactive site center of enzymes. Equally important is the ability of L-histidine in hemoglobin to buffer the H^+ ions from carbonic acid ionization in red blood cells.

Significant differences of antimicrobial activity of pure and metal ions doped L-histidine was found. The undoped L-histidine displayed very weak antibacterial activity against all types of microorganisms than the metal ions doped. However good antimicrobial activity was observed for all type of micro organisms with all type of metal ions doped L-histidine. It may be due to metal ions doped L-histidine the higher chance of electron delocalization between metal ions and imidazole ring than the undoped counterpart, were only limited electron delocalization took place within the ring only. This higher electron delocalization nature of metal ions doped L-histidine inhibits the growth of micro organisms most effectively. Again here also Cu^{2+} ions doped L-histidine exhibits greater range of inhibition than all the other metal ions. The corresponding findings are shown in Fig 7.

The sensitivity of the microorganisms against the pure and metal ions doped L-Histidine is represented as bar diagram and is shown in Fig 8.

Table 1: Comparison of unit cell parameters of grown crystals along with metal ions doped L-histidine.

	Pure L-Histidine	Na doped L-Histidine	K doped L-Histidine	Mg doped L-Histidine	Ni doped L-Histidine	Cu doped L-Histidine	Zn doped L-Histidine
hkl	(013)(102) (020)(123) (008)(018) (109)(119) (310)(229)	(004)(121) (016)(008) (119)	(004)(121) (015)(016) (116)(018) (018)(223) (041)(310)	(130)(220) (380)(461)	(120)(111) (162)(043)	(111)(250) (361)	(130)(320) (142)(023)
System	Orthorhombic	Orthorhombic	Orthorhombic	Orthorhombic	Orthorhombic	Orthorhombic	Orthorhombic
Space Group	$P2_12_12_1(19)$	$P2_12_12_1(19)$	$P2_12_12_1(19)$	$P2_12_12_1(19)$	$P2_12_12_1(19)$	$P2_12_12_1(19)$	$P2_12_12_1(19)$
Cell Parameters	a=5.143 b=7.294 c=18.674	a=5.143 b=7.294 c=18.674	a=5.143 b=7.294 c=18.674	a=8.976 b=16.16 c=6.963	a=8.944 b=15.30 c=6.838	a=8.944 b=15.30 c=6.838	a=8.976 b=16.16 c=6.963
Interfacial angles	$\alpha=\beta=\gamma=90^\circ$	$\alpha=\beta=\gamma=90^\circ$	$\alpha=\beta=\gamma=90^\circ$	$\alpha=\beta=\gamma=90^\circ$	$\alpha=\beta=\gamma=90^\circ$	$\alpha=\beta=\gamma=90^\circ$	$\alpha=\beta=\gamma=90^\circ$
JCPDS Card No.	51-2290	51-2290	51-2290	39-1855	31-1719	31-1719	39-1855

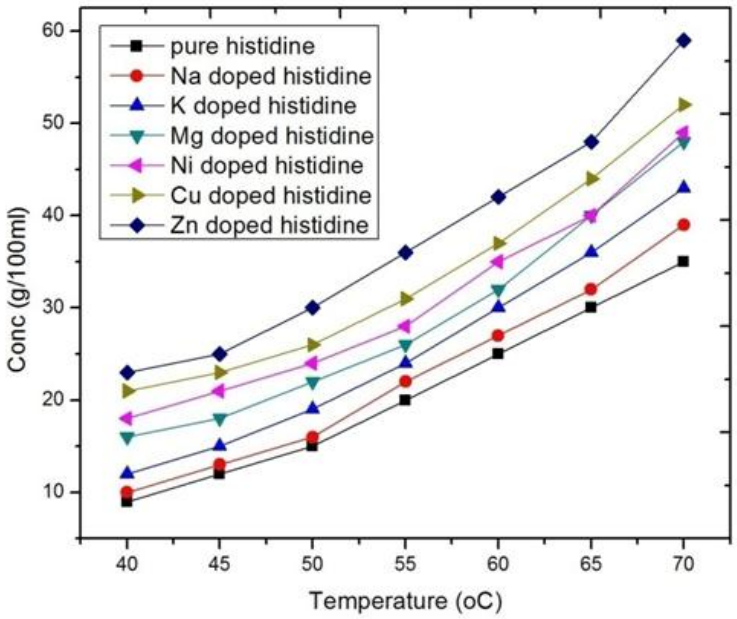

Fig 1 Solubility curve of pure and metal ions doped L-Histidine single crystals

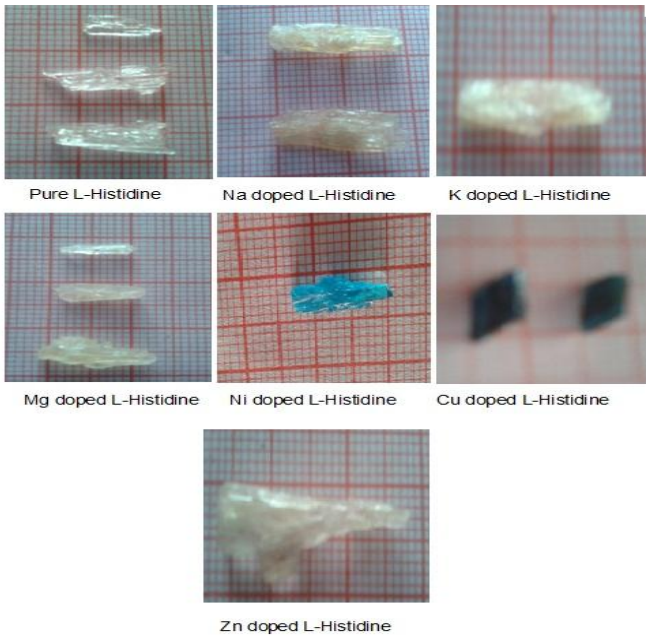

Fig 2 Photographs of pure and metal ions doped L-Histidine single crystals.

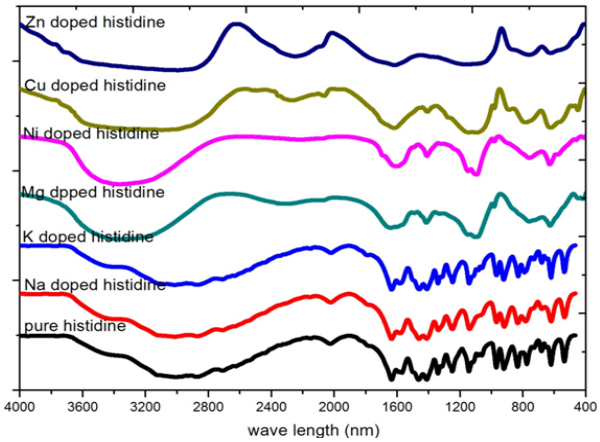

Fig 3 FTIR Spectra of pure and metal ions doped L-Histidine single crystals.

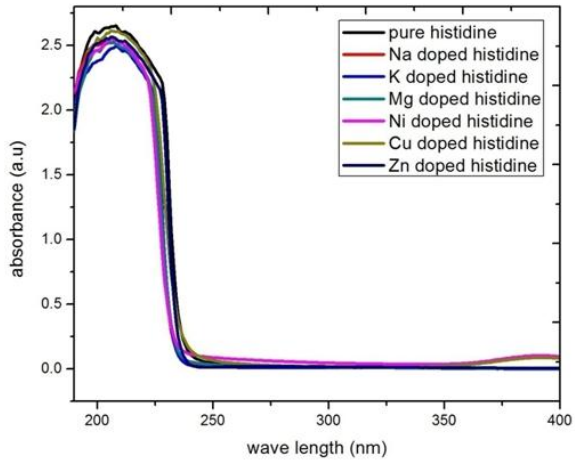

Fig 4 UV Spectra of pure and metal ions doped L-Histidine single crystals.

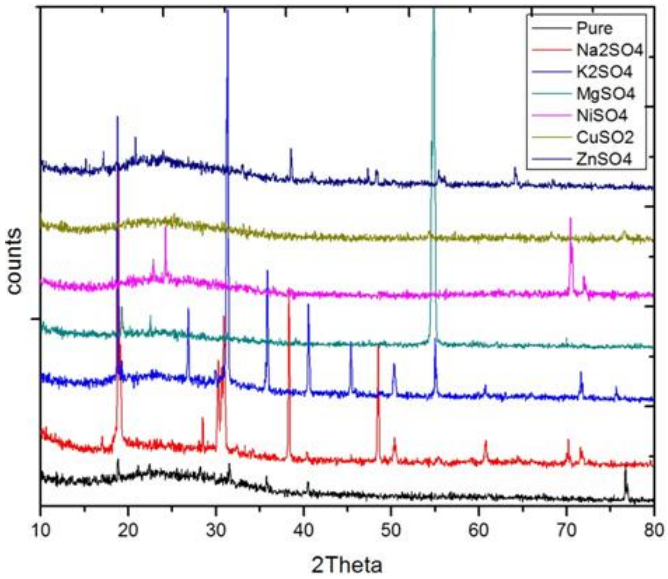

Fig 5 Powder XRD analysis of pure and metal ions doped L-histidine crystals.

Fig 6 Surface revealing of etched pure and metal ions doped L-Histidine single crystals.

.

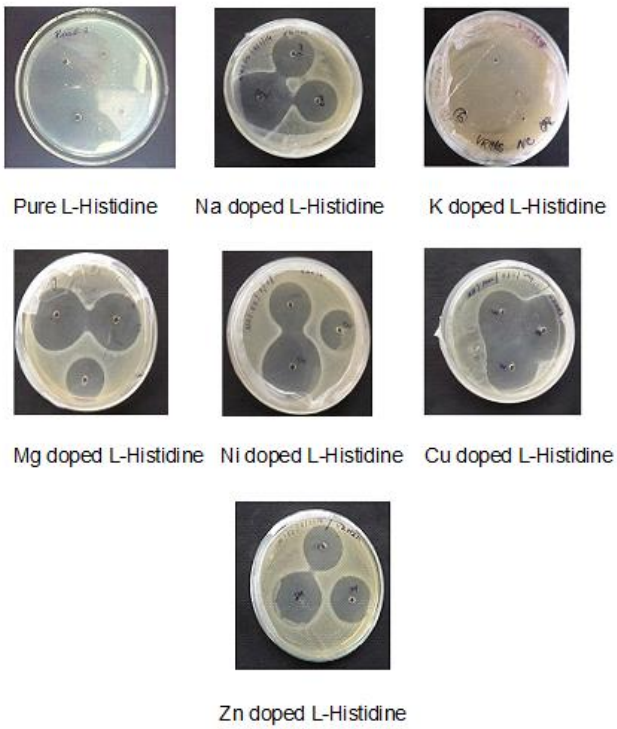

Fig 7 Antimicrobial activity of pure and metal ions doped L-Histidine single crystals.

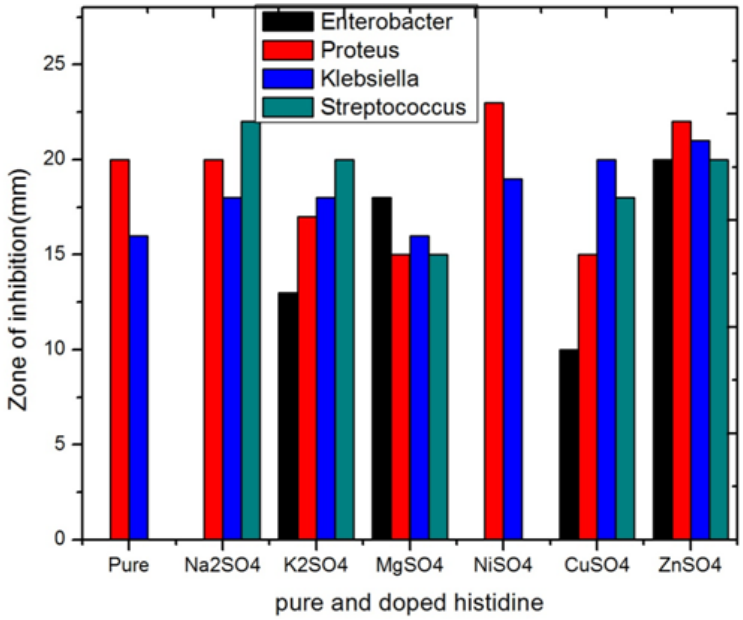

Fig 8 Zone inhibition areas of pure and metal ions doped L-Histidine single crystals.

4. Conclusion

The present study deals with growth of L-Histidine (basic), amino acid single crystals and alkali, alkaline earth and transition metal ions doped above said amino acid by using conventional slow evaporations solution growth method.

The functional groups present in the grown crystals were identified by recording FT-IR spectra. UV-visible spectra of pure and metal ions doped L-histidine crystals have a lower cut off wavelength is observed at 218 nm and 212 nm for pure and metal ions doped L-histidine crystals and this is due to π - π^* transition in the compounds.

The powder XRD study of L-histidine reveals that both metal ions doped and undoped L-histidine crystallizes in orthorhombic systems. The doping of metal ions on amino acid does not bring large distortion in L-histidine crystal and it allows retaining almost the single phase nature. In all doped samples, very little variation in the unit cell parameters is observed compared to pure L-histidine crystal, metal ions doped crystals were slightly distorted compared to pure L-histidine crystal. This might be attributed to strains on the lattice by the absorption of metal ions prior to L-histidine.

Among the numerous processes, which are influenced by crystallographic defects, there can be few situations in which the inter connections are as close as in the case of crystal growth. Crystallization both influences, and is influenced by, the defect structure of a crystal. Some of the dislocation pairs formed at isolated nucleation points originate at growth sector boundaries .In L-histidine the faceted growth is avoided so that the growth sectors will be reduced. Hence the dislocations which are associated with growth sector boundaries are absent in L-histidine grown crystal. This is the cause for low dislocation density in L-histidine grown crystal. Decrease in etch pits is associated with more systematic packing of the atoms/molecules and the strains formed during growth.

Significant differences of antimicrobial activity of pure and metal ions doped L-histidine was found. The undoped L-histidine displayed very weak antibacterial activity against all types of microorganisms than the metal ions doped ones. However good antimicrobial activity was observed among all type of micro organisms with all type of metal ions doped L-histidine. It may be due to metal ions doped L-histidine have the higher chance of electron delocalization between metal ions and imidazole ring than the undoped counterpart, were only limited electron delocalization took place within the ring only. This higher electron delocalization nature of metal ions doped L-histidine inhibits the growth of micro organism most effectively. Again here also Cu^{2+} ions doped L-histidine exhibit greater range of inhibition than all the other metal ions.

Acknowledgement

The author is thankful to University Grants Commission, New Delhi for providing financial assistance to carry out this work.

References

1. Mostad, A; Natarajan,S (1995); Kristallogr. Z; 210- 114.
2. Chemla D.S and Zyss,(Eds), J. (1987); *Nonlinear Optical Properties of Organic Molecule and Crystal*,Vol.**1** and vol.**2**, Academic Press,NewYork.
3. Vijayan, N; Bhagavannarayana, G; Nagarajan K. and Upadhya, V (2009), doi:10.1016/j.matchemphys. 2009.01.026.
4. Natarajan, S.; Shanmugam, G. and Martin Britto Dhas, S.A (2008). *Cryst. Res. Technol*, 43, No.5, 561-564/DOI 10.1002/crat.200711048.
5. Cruz-Vera, LR (2004). *"Ribosome stalling and peptidyl-tRNA drop-off during translational delay at AGA codons"*. *Nucleic Acid Research*. 32 **18**(15): 4462–8.
6. Reena Ittyachan,; Sagayaraj, P. (2003); *J. Cryst. Growth* 249 -557.
7. Rajendran, K.V; Jayaraman, D; Jayavel, R; Ramasamy, P (2003); *J. Crystal growth* 255 -361.
8. Vijayan, N; Bhagavannarayana, G; Nagarajan, K; Upadhyaya, V(2009); *Mater Chem. Phys.* 115-656.
9. Lucia Rose, A.S.J; Selvarajan, P; Perumal, S (2010); *Rec. Res. Sci. Tech*.2 (3): 76.
10. Nagamoto, K (1978). IR Spectra of Inorganic and Co ordination compounds (second edition) Wiley & Sons, New York.
11. Smith, B (1999). Infrared Spectral Interpretation: A Systematic Approach, CRC press, Washington, DC.
12. Kalsi, P.S (2002). Spectroscopy of Organic Compounds, New Age International Ltd, New Delhi.
13. Aruna, S; Anuradha, Preema, A; Thomas, C; Gulam Mohamed, M; RajaSekhar, S.A; Vimalan, M; Mani, G; and Sagayaraj, P(2007); *Indian Journal of pure and applied Physics*, 45:524.
14. Blaser ; Hans Ulrich (1992); "The chiral pool as a source of enantioselective catalysts and auxiliaries". *Chemical Reviews* **92** (5): 935–52.
15. Sanda Fumio; Endo; Takeshi (1999); "Feature Article Syntheses and functions of polymers based on amino acids". *Macromolecular Chemistry and Physics* **200** (12): 2651–61
16. Debye, P; Scherrer, P; *Physik. Z.* **27** (1917) 277.
17. Hull, A. W.; *Phys. Rev.* **(2)10** (1917) 84.
18. Hussaini, S.S; Datta, K; Ghosh, P.; Kadam,S.B.; Shirsat, M.D. ; *International Conf. on Optics and Photonics*, Chandigarh, India, 30 Oct- 1Nov(2009).
19. Parikh, K.D; Dave, D. J; Parekh, B.B; Joshi, M.J; *Cryst. Res. & Technol.* **10**(2010)1
20. Santosh, A. O; Gelamo, R. V; Li , B.B; Cardoso, L.P; Miranda, M.A.R; Nogueria, M.A.M; Remedios, C.M.R; Melo, A.E.A; Sasaki, J.M; Avanci, L.H; Morelhaa, S.L; *Mater. Res.* **4 (**2001) 43.
21. Kriss, T. C; Kriss, V. M; and *Vesna* M*; "*History of the Operating Microscope: From Magnifying Glass to Micro neurosurgery**,"** *Neurosurgery*, **42**(4), 899-907 (1998).
22. Ester, G. R ; Price, R ; Halfpenny, P.J ; *J. Phys. D: Appl. Phy,* 32A 128 (1999). DOI: 10.1088/0022-3727/32/10A/327